Mineralogical Magazine, February 2004, Vol. 68(1), pp. 177–189

Characterization of ammonioleucite $(NH_4)[AlSi_2O_6]$ and ND_4-ammonioleucite $(ND_4)[AlSi_2O_6]$ using IR spectroscopy and Rietveld refinement of XRD spectra

M. ANDRUT[1], D. E. HARLOV[2] AND J. NAJORKA[3]

[1] Institute for Mineralogy and Crystallography, University of Vienna - Geozentrum, A-1090 Vienna, Austria
[2] GeoForschungsZentrum Potsdam, Telegrafenberg, D-14473 Potsdam, Germany
[3] Corus Research, Development & Technology, Ceramics Research Centre, PO Box 10000, 1970 Ijmuiden, The Netherlands

ABSTRACT

Ammonioleucite, $(NH_4)[AlSi_2O_6]$, and its deuterated analogue ND_4-ammonioleucite $(ND_4)[AlSi_2O_6]$ have been synthesized in 20–150 mg amounts at 300ºC and 500 MPa in 5 mm wide, 4 cm long Au capsules using Rene' metal hydrothermal autoclaves. The resultant product consists of 20–30 μm-size single tetragonal crystals as well as 50–100 μm wide clumps of ingrown crystals. Infrared (IR) spectra obtained from powdered samples are assigned on the basis of T_d symmetry for both the ammonium and deutero-ammonium ion. They show triply degenerate vibrational bands (i.e. ν_3 and ν_4), some overtones, and combination modes from NH_4^+ and ND_4^+. While T_d symmetry for NH_4^+ in ammonioleucite is not strictly correct due to distortion of the NH_4^+ molecule, the non-cubic field is not large enough at room temperature to cause a substantial splitting in the bands. However, this perturbation is documented in the IR spectra by a substantial increase in the FWHH as well as the occurrence of shoulders on the broadened bands. In contrast, at lower temperatures, the observed band splittings in the former triply degenerated states of ν_3 and ν_4 could be explained by an effective local field with D_2 symmetry.

Rietveld refinement indicates that ammonioleucite, like leucite, has a tetragonal structure with space group symmetry $I4_1/a$. Here the NH_4^+ molecule replaces the K^+ cation on the 8-fold co-ordinated *W* site, which has *m* symmetry. Substitution of NH_4^+ for K^+ in the leucite structure results in an increase of the cell parameter *a*, whereas *c* is slightly reduced. The mean <W–O> bond length of ammonioleucite is increased in comparison to leucite from 3.00 to 3.12 Å whereas the mean <*T*–O> bond length of 1.65 Å remains unchanged. This results in an increase in the volume of the polyhedron hosting the NH_4^+ molecule as well as a decrease in distortion for structural channels parallel to the <111> direction, formed by the arrangement of the six-fold rings, on which the *W* cations are located. The same effect is also observed, in general, when Rb^+ or Cs^+ is substituted for K^+ in leucite.

KEYWORDS: ammonioleucite, IR spectroscopy, Rietveld refinement, XRD.

Introduction

AMMONIOLEUCITE, $(NH_4)[AlSi_2O_6]$, is the ammonium analogue of leucite where the NH_4^+ tetrahedron substitutes for K^+ on the 8-fold co-ordinated *W* site. Type ammonioleucite was first discovered as a coating of small crystals on analcime lining cavities in a hydrothermally altered greenschist located in Tatarazawa, Fujioka, Gunma Prefecture, Japan (Hori *et al.*, 1986). To date, the only other known natural occurrence of ammonioleucite has been identified in a hydrothermally altered MORB (Nishida *et al.*, 1997). While no mention is made of the oxidation state present during the hydrothermal alteration of these greenschists, it is highly likely that, like buddingtonite $(NH_4)[AlSi_3O_8]$ and

* E-mail: dharlov@gfz.potsdam.de
DOI: 10.1180/0026461046810179

tobelite $(NH_4)[AlSi_3O_{10}](OH)_2$ (Harlov *et al.*, 2001*a,b*), ammonioleucite is formed in a highly reducing, low-grade environment. It is also probable that one means by which it might be formed could be due to the hydrothermal alteration of leucite from circulating ammonia-enriched groundwaters which are also in contact with organic-rich black shales, coal deposits and/or oil deposits. Like leucite, ammonioleucite is tetragonal with $I4_1/a$ space group symmetry (Hori *et al.*, 1986). So far, ammonioleucite has not been synthesized. Past attempts at characterization have only been made for the type material, natural ammonioleucite $(NH_4,K)[AlSi_2O_6]$, as described by Hori *et al.* (1986). These include powder X-ray diffraction (XRD) data as well as infrared (IR) absorption spectra though no attempt has been made to assign transitions to any of the observed bands. Yamada *et al.* (1998) applied the Rietveld refinement method to an XRD pattern taken from the same sample of type ammonioleucite, which contains a substantial K^+ component of ~20 mol.% in contrast to the synthesized ammonioleucite in this study which is pure end-member.

In this study we have synthesized both ammonio- and ND_4-ammonioleucite for the purposes of characterization and comparison of their crystal chemistry using both IR absorption powder spectroscopy down to 77 K as well as Rietveld refinement of powder XRD spectra. Such a study provides a useful comparison with similar studies of buddingtonite and ND_4-buddingtonite (Harlov *et al.*, 2001*a*) as well as NH_4-analcime (Likhacheva *et al.*, 2002). It is intended that this study will also serve as a basis for future investigations of the ND_4^+ molecule in the ammonioleucite structure using more sophisticated techniques such as neutron diffraction and NMR at temperatures below 77 K.

Experimental procedure

Synthesis

Ammonioleucite was synthesized in 20–150 mg amounts using a stoichiometric Al_2O_3-SiO_2 mix and a 25% NH_3 solution in excess such that the amount of NH_4^+ available was 50% greater than needed stoichiometrically. The Al_2O_3-SiO_2 mix consisted of grinding the α-Al_2O_3 and SiO_2 (weighed out to ±0.05 mg) together in 1 g batches in ethanol for 30 min such that they were completely homogenized. Synthesis consisted of placing 20–150 mg of the dry oxide mix along with 150 mg of 25% NH_3 solution into either 3 mm wide, 2 cm long or 5 mm wide, 4 cm long Au capsules with wall thickness of 0.2 mm. The Au capsule, partially immersed in an icewater bath, was then welded shut using an argon plasma torch. The sealed capsule was placed in a 6 mm diameter bore, cold-seal Rene' metal, hydrothermal autoclave with a Ni-NiO filler rod and an external NiCr thermocouple. The synthesis run was then taken up to 300ºC and 500 MPa for ~1 week. Temperatures were monitored continuously and are believed to be accurate to within ±3ºC. Pressure was measured using a pressure transducer calibrated against a Heise gauge manometer for which the quoted pressure is accurate to ±5 MPa. The synthesis run was quenched using compressed air. This ensured that the interior of the autoclave cooled to <100ºC within 2–3 min of initial quench. In a successful synthesis run, the resultant product consisted of ammonioleucite in the form of 20–30 μm size single tetragonal crystals (Fig. 1*a,b*) as well as 50–100 μm wide clumps of intergrown crystals (Fig. 1*c,d*). Impurities included minor quartz, buddingtonite and tobelite. The centre of these clumps are rich in fluid inclusions indicating rapid nucleation surrounded by very clear inclusion-free thick rims indicating later slower growth; similar to what has been seen in synthetic buddingtonite (cf. Harlov *et al.*, 2001*a*, their Fig. 1*d*).

Synthesis of ND_4-ammonioleucite was carried out in much the same way, here at 500ºC and 500 MPa. The principal difference was the use of a 26% solution of ammonium deuteride, i.e. ND_3 in D_2O. Other differences included using a new dry syringe for loading the 26% ND_3 solution into the Au capsule previously dried at 105ºC overnight and synthesis runs of only one week. This was done to minimize H/D exchange with the external pressure medium (H_2O). One week was necessary to ensure complete crystallization of the ND_4-ammonioleucite. Even so, IR spectroscopy indicated a significant ammonioleucite component in each of the three ND_4-ammonioleucite synthesis runs (see below).

IR spectroscopy

The synthesized crystals of ammonio- and ND_4-ammonioleucite were too small to allow for single-crystal measurements (Fig. 1), and so only powdered samples could be investigated. The FTIR samples were prepared by grinding

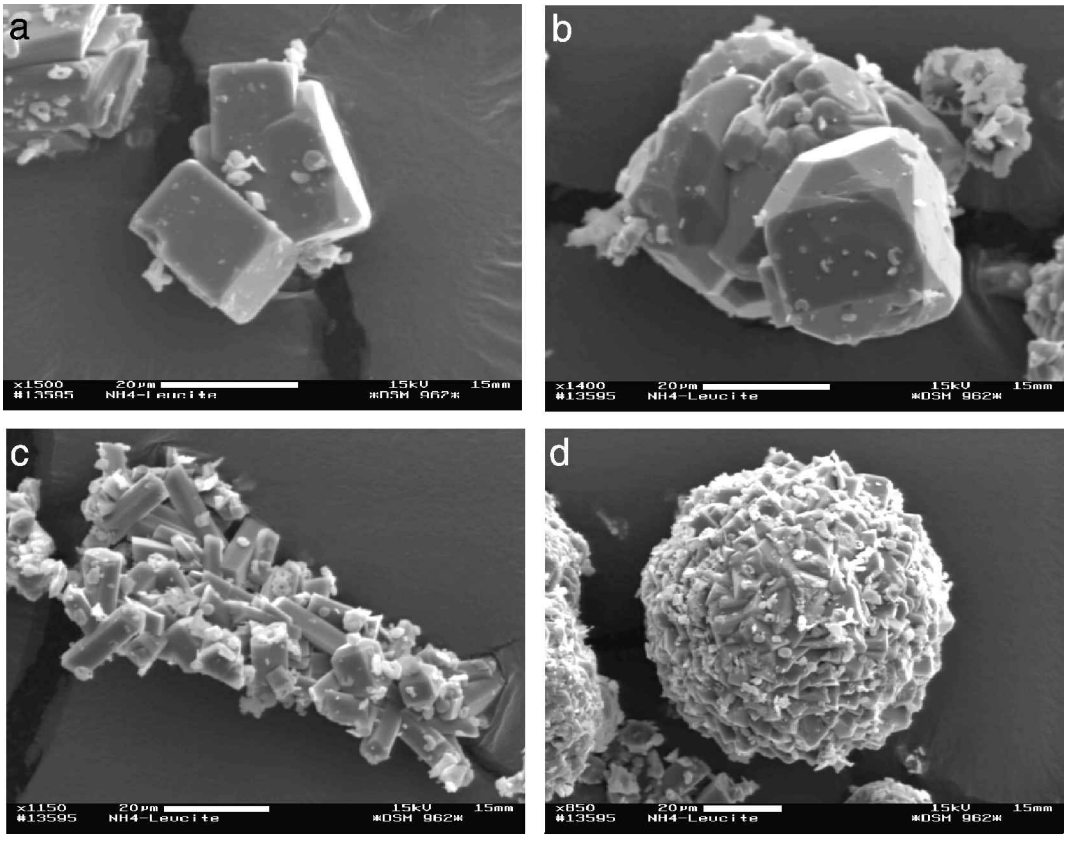

FIG. 1. (*a,b*) SEM photographs of individual ammonioleucite crystals showing tetragonal symmetry at different orientations with respect to the *c* axis. (*c,d*) SEM photographs of a typical clump of intergrown ammonioleucite crystals which were also common for synthesis runs.

5 mg of ammonio- or ND_4-ammonioleucite and dispersing it in 450 mg of KBr. The homogenized mixture was pressed into 13 mm diameter transparent pellets under vacuum and then dried for several days at 170ºC. No recognizable difference was seen between the IR spectrum of a powdered sample taken using an IR microscope as compared to a sample dispersed in a prepared KBr pellet. This indicates that no measurable exchange between the K in the KBr and the NH_4^+ or ND_4^+ in the ammonioleucite took place. Absorption measurements were carried out in the spectral range 3800 cm^{-1} to 350 cm^{-1} with a resolution of 2 cm^{-1} using a Bruker IFS 66v/S FTIR spectrometer equipped with a globar as the light source, a KBr-beam splitter and DTGS-detector. Spectra were averaged over 256 scans. Phase correction mode of the interferogram was performed using the procedure after Mertz (1965) (Griffiths and de Haseth, 1986). Norton-Beer-weak mode was chosen as the apodization function. The sample chamber of the Bruker IFS 66v was evacuated down to 200 Pa. Therefore the influence of H_2O vapour and CO_2 is negligible. In order to study their behaviour at low temperature, samples were cooled to 77 K in the FTIR spectrometer using liquid N_2 in an internal cooling device. The resulting spectra are displayed as a function of the wavenumber. After background correction, the band centre, full width at half height (FWHH) and integral intensity of each absorption band were determined using the program *PeakFit*© by Jandel Scientific. The IR spectra for both the ammonioleucite and ND_4-ammonioleucite are given in Table 1 and in Figs 2–4.

TABLE 1. Band assignments for vibrational modes (ν) with respect to centre, FWHH (FW) in cm^{-1} and relative intensity (Int).

ν (cm^{-1})	$(NH_4)^+$	NH_4Cl (298 K)**			Buddingtonite B3 (298 K)**			Ammonioleucite N-H vib. (298 K)			Ammonioleucite N-H vib. (77 K)			ND_4-ammonioleucite N-D vib. (298 K)			ND_4-ammonioleucite N-D vib. (77 K)		
	Centre	Centre	FW	Int	Centre	FW	Int	Centre	FW	Int	Centre	FW	Int	Centre	FW	Int	Centre	FW	Int
ν_4	1400	1400	25	s	1440	60	m	1430	45	m	1425 sh	20	m	n.o.			n.o.		
					1480 sh		w	1470 sh		w	1445	25	m	n.o.			n.o.		
											1475	30	m	n.o.			n.o.		
ν_2	1680*																		
$2\nu_4$		2810	100	w	2845	130	m	2890	130	m	2840	90	m	2150	80	w	2150	65	w
								2930 sh		w	2910	50	w						
$\nu_2+\nu_4$, ν_1[a]		3015	130	m	3045	220	m	3045	190	m	3040	200	m	2280	70	m	2280	60	m
$2\nu_2$					3180 sh		w	3180 sh		w	3140 sh		w	2345	70	m	2345	55	m
ν_3	3145	3140	130	s	3295	240	s	3260	190	s	3220 sh		w	2400	70	m	2395	80	m
											3260	190	m	2460 sh			2465 sh		

sh – shoulder; w – weak; m – medium; s – strong; n.o.– not observed, * = Raman active.
**Harlov *et al*. (2001*a*); [a] = ν_1 is Raman active in T_d

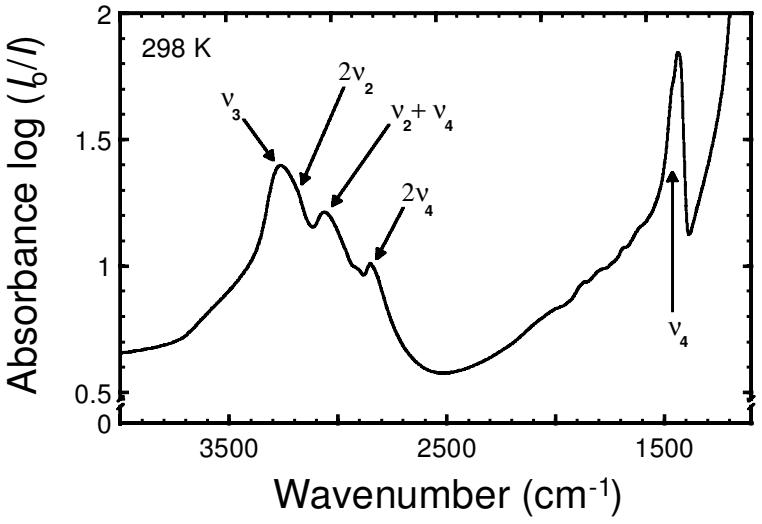

FIG. 2. Normal modes, on the basis of T_d symmetry, for IR spectra of ammonioleucite at 298 K. See text and Table 1 for a description of the various band assignments.

Electron microprobe analysis

The synthesized ammonioleucite was analysed using a JEOL JXA 8900-RL microprobe at the Geowissenschaftliches Zentrum der Universität Göttingen. Ammonioleucite crystal clumps, 40–60 μm in diameter, were mounted in epoxy and polished. The sample was then coated with a 120 Å thick carbon coating. All analyses were performed using a 10 keV, 15–20 nA, 3 μm beam spot. In order to minimize carbon deposition on the measured spot, a plate, cooled by liquid N_2, was situated 2 mm above the grain mount in order to freeze out carbon-containing volatiles from the diffusion pump oil etc. N_2 was counted on a multilayer LDEN crystal which has ten times the sensitivity for N_2 than the more common PC1 (= LDE1) crystal. Standards included natural orthoclase for O_2, Si and Al and synthetic buddingtonite for N_2 (Harlov *et al.*, 2001*a*). Counting times were 20 s for N_2 and 16 s for the other elements.

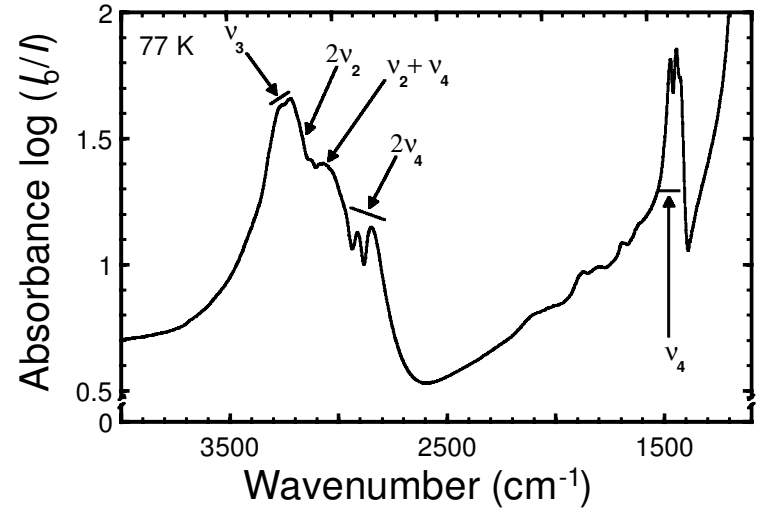

FIG. 3. Normal modes, on the basis of T_d symmetry, are given for spectra of synthetic ammonioleucite at 77 K. See the text and Table 1 for a description of the various band assignments.

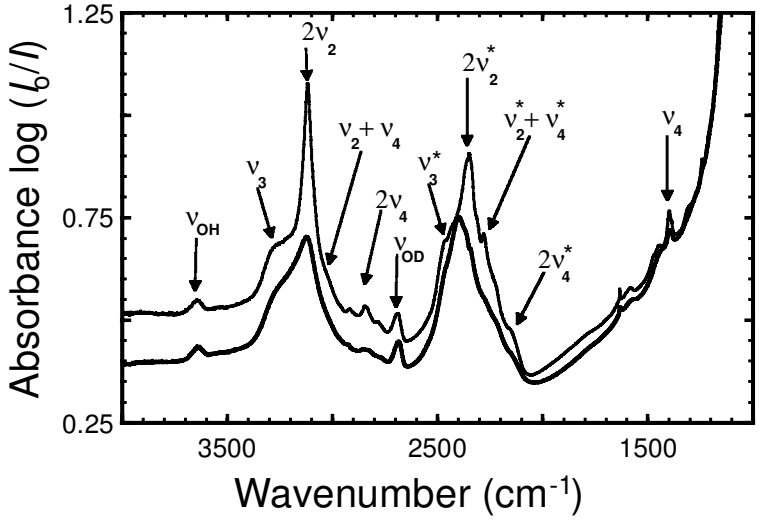

FIG. 4. Normal modes, on the basis of T_d symmetry, are given for spectra of synthetic ND_4-ammonioleucite at 298 K (bold line) and 77 K (light line). Additional absorption bands due to N-D vibrations are marked with an asterix. See the text and Table 1 for a description of the various band assignments.

Ammonioleucite analyses are listed in Table 2. These analyses suggest that the synthetic ammonioleucite is stoichiometric and contains no appreciable amounts of zeolitic H_2O.

X-ray analysis

Determination of phases present in the charge was accomplished using powder X-ray diffraction analysis. For this purpose 1 or 2 mg of the charge were ground in an agate mortar to a grain size of <2 μm. The powder was diluted with Elmer's White Glue© and mounted on a circular foil. Powder XRD patterns were recorded in transmission using a fully automated STOE STADI P diffractometer (Cu-$K\alpha_1$ radiation) equipped with a primary monochromator and a 7°-position sensitive detector. Operating conditions were 40 kV and 40 mA with a take off angle of 6°. The spectra were recorded in the range of 5 to 125° (2θ) using a step interval of 0.1°. The resolution of the PSD was set to 0.02°. Counting times were selected to yield a maximum intensity of ~3300 counts for each sample, resulting in 5 to 20 s per detector step. Unit-cell dimensions, additional structural parameters, and quantitative phase analysis were determined using the Rietveld analysis technique contained in the GSAS software package (Larson and Von Dreele, 1987).

For starting values in the Rietveld refinement of ammonioleucite, we chose the unit-cell parameters, atomic co-ordinates and isotropic displacement factors given by Yamada *et al.* (1998) for the tetragonal structure ($I4_1/a$) of a natural (NH_4,K)-ammonioleucite. The distribution of the Al and Si on the tetrahedral sites was assumed to be disordered, in accordance with the results of Yamada *et al.* (1998). The Al/Si ratio at the tetrahedral sites was fixed to 0.33/0.67, with respect to the chemical formula as determined by microprobe analysis. The occupancy factor for the

TABLE 2. Microprobe analyses of synthetic ammonioleucite.

Analysis	1	2	3	4	5
$(NH_4)_2O$	12.40	12.94	13.31	12.57	12.38
SiO_2	60.03	61.14	61.31	59.00	60.84
Al_2O_3	25.05	25.60	24.32	27.53	24.41
Total	97.48	99.70	98.94	99.10	97.68
Atoms p.f.u. *					
$^{IX}NH_4$	0.96	0.98	1.02	0.96	0.96
^{IV}Si	2.02	2.01	2.03	1.95	2.04
^{IV}Al	0.99	0.99	0.95	1.07	0.96

*calculated on the basis of 6 oxygen atoms

ammonium ion was set to 1, based on microprobe analysis (Table 2). The assumption of ideal stoichiometry is also confirmed by the results of IR spectroscopy, which gave no indication of molecular water in the structure unlike what was observed for type ammonioleucite (Yamada *et al.*, 1998). The scattering factor and isotropic displacement factor of N used for the ammonium ion was taken from Yamada *et al.* (1998). Starting values for minor tobelite and buddingtonite, appearing in each of the ammonioleucite syntheses, were taken from Harlov *et al.* (2001*a,b*). The number of profile parameters used was 21. These consisted of 16 parameters to fit the background using a real space correlation and 5 parameters to define the peak form as a pseudo-Voigt with a variable Lorentzian character. No parameters describing peak asymmetry were necessary, because the peak shape is highly symmetric due to the geometry of the STOE STADI P diffractometer. The preferred orientation for ammonioleucite was corrected using the formulation of March (1932) and Dollase (1986). The following sequence was used for the refinement procedure: scale factor, background, zero-point correction, phase fractions, lattice constants, Caglioti W, preferred orientation, atomic positions, Caglioti U+V, Lorentz LX+LY. The atom fractions and isotropic displacement factors were not refined. The XRD pattern and corresponding Rietveld refinement for ammonioleucite and ND_4-ammonioleucite synthesis runs are shown in Fig. 5 and summarized in Tables 3–5.

Results and discussion

IR spectroscopy

Band positions and FWHH for ammonioleucite and ND_4-ammonioleucite are summarized in Table 1, and compared with data obtained for

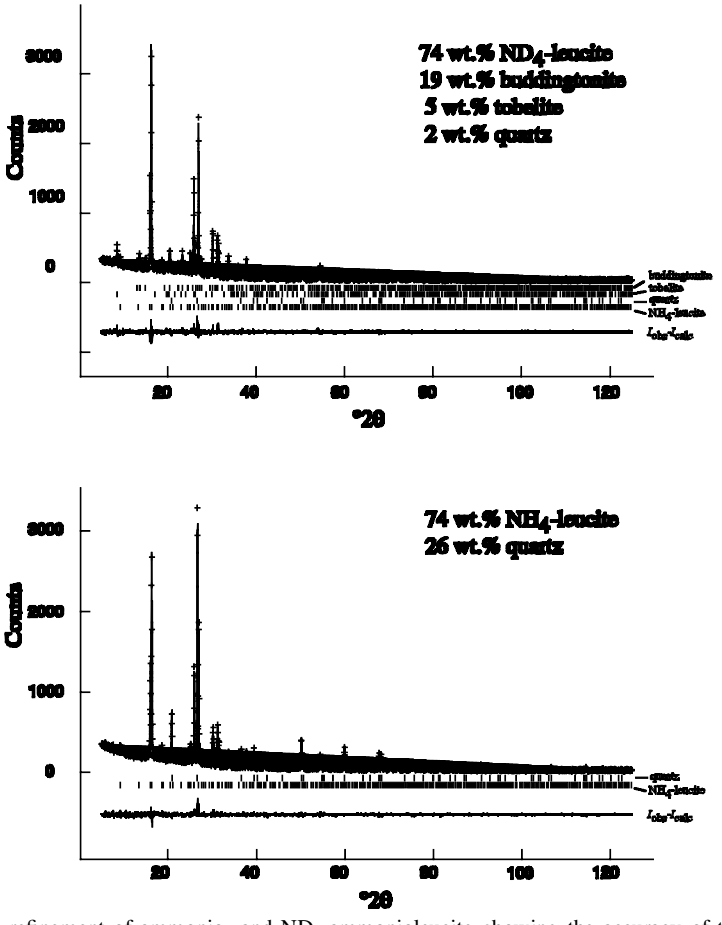

FIG. 5. Rietveld refinement of ammonio- and ND_4-ammonioleucite showing the accuracy of the refinement.

TABLE 3. Refinement details.

Sample	R_p	R_{wp}	χ^2	DW	Phase proportions (wt.%)
Ammonioleucite	0.11	0.08	1.20	1.70	74 ammonioleucite, 26 quartz
(ND_4)-ammonioleucite	0.12	0.09	1.52	1.33	74 ND_4-ammonioleucite, 19 ND_4-buddingtonite, 5 ND_4-tobelite, 2 quartz

synthetic buddingtonite (Harlov *et al.*, 2001*a*). The free ammonium ion has T_d symmetry giving rise to four normal vibrational modes (Herzberg, 1955). These have the representations A_1 (ν_1), E (ν_2), and $2 \times T_2$ (ν_3 and ν_4). All fundamentals are Raman active, but only the triply-degenerated ν_3 and ν_4 modes are IR active. The fundamental frequencies for the free ammonium ion are ν_1 = 3040 cm^{-1}, ν_2 = 1680 cm^{-1}, ν_3 = 3145 cm^{-1} and ν_4 = 1400 cm^{-1} (Nakamoto, 1986, after Landolt-Börnstein, 1951). In accordance with selection rules for T_d symmetry, under ambient conditions the IR spectrum of NH_4Cl contains two intense absorption bands which can be assigned to the triply degenerate vibrations ν_3 (N-H stretching) and ν_4 (N-H-N bending) of the NH_4^+ molecule (Wagner and Hornig, 1950). Additionally, at the low-energy wing of the stretching band, ν_3, a combination mode $\nu_2+\nu_4$ and the first overtone of the ν_4 bending mode are clearly visible. A decrease in the local symmetry of the ammonium ion may lead to a splitting of the former degenerate states, resulting in further absorption bands (Beran *et al.*, 1992). Due to similarities in the local environment for the ammonium ion in both the leucite and feldspar structures, the behaviour of the NH_4^+ molecule in buddingtonite at room temperature (Harlov *et al.*, 2001*a*) can help to explain the IR absorption spectrum of both ammonioleucite and its deuterated analogue. In addition, recent IR results obtained for NH_4-analcime by Likhacheva *et al.* (2002) are taken into account. Those authors determined the type and symmetry of the NH_4^+ ion with respect to the number of split components for the ν_4 bending mode (after Burgina *et al.*, 1986).

The IR spectra for ammonioleucite at ambient conditions and 77 K are given in Figs 2 and 3, respectively. The IR spectra for ND_4-ammonioleucite at 298 and 77 K are displayed in Fig. 4. Ammonioleucite shows a broad band around 1430 cm^{-1} and a system of overlapping bands in the spectral region 2700 to 3500 cm^{-1}. These absorption bands are attributed to the presence of NH_4^+. ND_4-ammonioleucite additionally exhibits a system of bands around 2850 to 2200 cm^{-1}, which are due solely to the presence of ND_4^+ (Fig. 4). Because the spectrum of ND_4-ammonioleucite shows absorption bands due to both N-D and N-H vibrations, it is concluded that during synthesis, substantial diffusion of H_2 took place through the capsule. While vibrations due to the ND_4^+ molecule are shifted to a lower energy as compared to those for NH_4^+ (Fig. 4 and Table 1), they still show the same basic pattern of absorption bands. Partly deuterated samples could also give rise to ND_xH_{4-x} species (Oxton *et al.*, 1975, 1976); however, only two main broad band systems are observed. Minor tobelite in the ND_4-ammonioleucite synthesis shows up in the IR-absorption spectra as bands due to OH- and OD-stretching vibrations at 3640 cm^{-1} and 2685 cm^{-1}, respectively (Harlov *et al.*, 2001*b*). Its bands, due to NH_4^+ and ND_4^+, are superimposed upon the NH_4^+ and ND_4^+ bands of ammonioleucite. The presence of tobelite in this particular sample was also confirmed by Rietveld analysis (cf. Table 3).

The tetrahedral NH_4^+ ion is situated on the *W* site in the ammonioleucite structure, which has *m*-site symmetry and eightfold co-ordination. In the crystal field of ammonioleucite the symmetry of the NH_4^+ molecule is reduced and causes a further splitting of the formerly degenerate energy levels (Bastoul *et al.*, 1993). Further evidence of a symmetry reduction has been described by Beran *et al.* (1992) from their IR single crystal study of a NH_4^+-bearing hyalophane crystal from Zargrlski Potok, Bosnia, which shows both a splitting and a polarization behaviour in the N-H vibrational bands. This perturbation of the NH_4^+ molecule is documented in the IR spectra of ammonioleucite by a substantial increase in the FWHH of the vibrational bands caused by NH_4^+, in contrast with its T_d symmetry in NH_4Cl (cf. Table 1; Harlov *et al.*, 2001*a*). It is also documented by the occurrence of shoulders on the broadened bands and splitting into components of former degenerated states; well demonstrated in case of the

TABLE 4. Results of Rietveld analysis of X-ray powder data (λ = 1.541221).

	Ammonioleucite				ND_4-ammonioleucite			
(h k l)	d (Å)	º2θ	I/I_{100}(obs)	I/I_{100}(cal)	d (Å)	º2θ	I/I_{100}(obs)	I/I_{100}(cal)
1 0 1	9.528	9.27	3.1	3.0	9.532	9.27	2.8	3.5
2 0 0	6.615	13.38	1.4	1.2				
1 1 2	5.536	16.00	44.9	43.8	5.539	15.99	36.8	38.4
2 1 1	5.434	16.30	100.0	100.0	5.433	16.30	100.0	100.0
2 0 2	4.764	18.61	5.1	4.4	4.766	18.60	4.5	4.4
2 1 3	3.621	24.57	1.6	1.5	3.623	24.55	1.2	1.2
3 2 1	3.545	25.10	9.6	9.7	3.544	25.11	10.0	9.4
0 0 4	3.434	25.93	49.7	43.5	3.438	25.90	42.2	40.0
4 0 0	3.307	26.94	71.2	66.3	3.306	26.95	65.4	61.8
3 0 3	3.176	28.07	2.2	2.0	3.177	28.06	2.6	2.2
4 1 1	3.125	28.55	3.3	3.7	3.124	28.56	3.4	3.5
2 0 4	3.048	29.28	3.3	3.2	3.050	29.26	3.1	2.9
4 0 2	2.980	29.97	2.7	2.5	2.980	29.97	2.7	2.4
4 2 0	2.958	30.19	19.8	18.1	2.957	30.20	19.6	18.2
3 2 3	2.863	31.22	21.6	19.2	2.864	31.21	20.5	18.1
3 3 2	2.839	31.49	13.9	12.9	2.839	31.49	15.3	13.2
4 2 2	2.717	32.94	1.2	1.0	2.717	32.95	1.0	1.0
3 1 4	2.654	33.75	8.5	8.1	2.656	33.73	7.2	7.4
4 1 3	2.628	34.10	2.2	2.1	2.628	34.09	2.3	2.2
2 1 5	2.492	36.02	5.4	5.1	2.494	35.99	5.3	5.3
5 1 2	2.427	37.01	3.9	3.4	2.427	37.02	3.8	3.4
5 2 1	2.418	37.15	1.5	1.4	2.417	37.16	1.3	1.2
4 0 4	2.382	37.74	9.2	9.2	2.383	37.72	8.8	8.2
4 4 0	2.339	38.46	1.7	1.7	2.338	38.48	1.5	1.6
1 1 6	2.224	40.54	1.0	1.1				
5 2 3	2.165	41.69	1.9	1.7	2.165	41.70	1.9	1.5
2 0 6	2.163	41.72	2.8	2.5	2.165	41.68	3.1	2.5
5 3 2	2.154	41.90	2.7	2.4	2.154	41.91	2.9	2.5
6 1 1	2.148	42.03	2.7	2.2	2.147	42.05	2.3	2.1
6 2 0	2.092	43.22	2.1	1.8	2.091	43.24	2.1	2.0
5 4 1	2.043	44.30	2.9	2.6	2.042	44.32	2.5	2.7
6 2 2	2.001	45.29	1.0	1.0	2.001	45.30	1.1	0.9
6 3 1	1.952	46.49	2.8	2.6	1.951	46.50	2.3	2.1
5 4 3	1.883	48.29	2.3	2.1	1.883	48.30	2.1	2.1
4 0 6	1.882	48.32	2.3	2.1	1.884	48.28	2.0	2.0
3 3 6	1.845	49.35	2.1	1.8	1.846	49.32	1.7	1.8
6 4 0	1.835	49.66	2.0	1.9	1.834	49.68	1.7	1.8
6 3 3	1.811	50.34	1.6	1.4	1.811	50.35	1.5	1.4
4 2 6	1.810	50.37	1.4	1.3	1.811	50.34	1.4	1.3
5 5 2	1.805	50.52	1.4	1.4	1.805	50.54	1.6	1.6
7 2 1	1.802	50.63	1.0	1.0	1.801	50.65	1.0	1.0
7 0 3	1.747	52.33	1.8	1.4	1.747	52.34	1.3	1.3
3 2 7	1.730	52.88	3.9	4.1	1.732	52.83	3.4	3.7
0 0 8	1.717	53.32	1.1	1.0				
6 1 5	1.705	53.72	1.4	1.1	1.706	53.70	1.3	1.0
7 2 3	1.689	54.27	2.7	2.6	1.689	54.28	2.8	2.6
7 3 2	1.684	54.44	8.3	8.1	1.684	54.46	7.7	7.6
4 1 7	1.674	54.80	2.1	2.0	1.675	54.76	1.6	2.0
2 0 8	1.662	55.24	1.2	1.0	1.664	55.17	1.0	1.1
7 1 4	1.643	55.93	2.7	2.5	1.643	55.93	2.5	2.4
8 2 0	1.604	57.39	2.5	2.4	1.604	57.42	2.7	2.8
3 1 8	1.588	58.03	1.7	1.8	1.590	57.97	1.3	1.6
7 3 4	1.550	59.60	1.8	1.6	1.550	59.61	2.0	1.7

TABLE 5. Refined lattice constants.

Sample	*a* (Å)	*c* (Å)	*V* (Å^3)	Source
Ammonioleucite	13.2296(7)	13.7348(9)	2403.9(3)	This study
(ND_4)-ammonioleucite	13.2245(6)	13.7509(8)	2404.9(3)	This study
Ammonioleucite	13.1700	13.6900	2374.5	Barrer *et al.* (1953)
(NH_4,K)-ammonioleucite	13.2140	13.7130	2394.4	Hori *et al.* (1986)*
(NH_4,K)-ammonioleucite	13.2106(6)	13.7210	2394.6	Yamada *et al.* (1998)**
Leucite	13.0548(2)	13.7518(2)	2343.69(1)	Palmer *et al.* (1997)***

*, ** natural samples from Tatarazawa, Fujioka, Japan
* composition $[(NH_4)_{0.68}K_{0.19}]_{0.87}Al_{0.89}Si_{2.12}O_6$
** composition $[(NH_4)_{0.53}K_{0.34}]_{0.87}Al_{0.89}Si_{2.12}O_6$
*** natural leucite from Roman Volcanic Province, Italy, composition $K_{0.97}Al_{1.01}Si_{1.99}O_6$

bending mode ν_4 at 77 K (Table 1 and Fig. 2). This indicates that the T_d symmetry is no longer valid, at least at lower temperatures around 77 K. As in buddingtonite (Harlov *et al.*, 2001*a*), the FWHH of both the ν_3 and $2\nu_2$ bands are nearly twice as large as those for NH_4Cl. Several studies have shown that the fundamental ν_4 is highly sensitive to distortion of the ammonium ion (e.g. Oxton *et al.*, 1975, 1976). Under ambient conditions, this mode is exhibited in the spectrum of ammonioleucite as a weak shoulder, but clearly shows three components (1425, 1445 and 1475 cm^{-1}) at 77 K. Similarly at 77 K, the overtone $2\nu_4$ exhibits two well resolved components, while its third component is hidden under the $\nu_2 + \nu_4$ combination mode. Further bands arise from overtones ($2\nu_2$ and $2\nu_4$) and a combination mode ($\nu_2 + \nu_4$). These are superimposed on the spectrum, which is due to the triply degenerate transitions ν_3 and ν_4. Therefore the labelling according to T_d symmetry in Figs 2 and 4 should be viewed as an approximation. At 77 K the splitting of band ν_3 may also contribute to the band broadening, giving rise to two peaks at 3260 and 3220 cm^{-1}. Weak spectral features in the spectral range 1600 to 2100 cm^{-1} are overtones of Si-O and Al-O vibrations, which are visible due to the large amount of sample material used (5 mg).

While the room-temperature spectrum of ammonioleucite is more similar to that of buddingtonite, the low-temperature spectrum is nearly identical to that of NH_4-analcime at the same temperature (Likhacheva *et al.*, 2002). Nevertheless, the symmetry reduction proposed by the authors to explain the observed band splitting cannot be adopted in the case of ammonioleucite and ND_4-ammonioleucite. Taking into account all possible subgroups of T_d for the NH_4^+-ion, D_2 symmetry is the only one that properly describes the observed splitting scheme. According to the symmetry correlation, the former triply degenerate state T_2 (ν_3 and ν_4) split into three components $B_1 + B_2 + B_3$, which are all IR-active. The representations for ν_1 and ν_2, (A_1 and E, respectively) transform according to A and A + A, but remain IR inactive.

In the case of all other subgroups of T_d that correctly describe the lifting of the triply degenerated states into three one-dimensional representations (C_{2v}, C_2, C_s and C_1), the fundamentals ν_1 and ν_2 become IR active, while the E mode will split into two components (except for C_3).

Values for the free ammonium ion (Nakamoto, 1978) suggest that the energies for these transitions are shifted slightly to higher energies, i.e. at ~3050 cm^{-1} and 1700 cm^{-1}. Indeed, in the case of NH_4-analcime, Likhacheva *et al.* (2002) assigned a band at 3060 cm^{-1} to the ν_1 transition on the basis of their symmetry reduction scheme. Nevertheless, for all of the symmetry models discussed (C_{3v}, C_{2v}, C_s and C_1), no band was found in this spectral range that could be assigned to the ν_2 transition.

In the present low-temperature spectrum for ammonioleucite, a possible ν_1 transition could be superimposed by the $\nu_2 + \nu_4$ combination mode (see Table 1). Nevertheless, the fundamental ν_2 should be clearly visible in case it is IR active and thus show a distinctive strong peak among the spectral features in the vicinity of 1700 cm^{-1}

(compare also to the spectra given in Oxton *et al.* (1975)).

The relative degree of hydrogen bonding between the NH_4^+ molecule and the surrounding oxygens in ammonioleucite can be estimated from comparison with the ammonium halides (e.g. NH_4Cl) and buddingtonite. In the ammonium halides the N-H-*X* hydrogen bonds are extremely weak. The N-H frequency is typically ~3300 cm^{-1}. The deformation mode ν_4, which can be used as a clear indicator for the formation of hydrogen bonds, is generally shifted to higher energies (Plumb and Hornig, 1950). Absorption bands due to hydrogen bonding in ammonioleucite are found at ~3260 and 1430 cm^{-1} (Fig. 2) and are comparable to similar energies reported for buddingtonite (Harlov *et al.*, 2001*a*) and analcime (Likhacheva *et al.*, 2002). The position of these absorption bands represents only a slight shift (30 cm^{-1}) in the stretching and deformation modes to higher energies. As in buddingtonite, this weak shift implies that hydrogen bonding between the NH_4^+ molecule and the surrounding oxygens is relatively weak if non-existent in ammonioleucite. In the case of ND_4-ammonioleucite, as in ND_4-buddingtonite, ν_4* is hidden under the Si-O stretching modes.

The IR spectrum for ammonioleucite at ambient conditions shows no pronounced splitting of the N-H bands (compare Figs 2 and 4), and only a weak shoulder for the band ν_4 comparable to buddingtonite. This implies that a detailed description of the effective symmetry for the ND_4^+ ion and the NH_4^+ ion is not possible from IR spectra at room temperatures. Therefore, within the scope of this study, this justifies assigning the most intense N-H and N-D bands to vibrational transitions on the basis of T_d symmetry as a first approximation (Table 1). However, the low-temperature spectrum revealed a significant splitting of the fundamental ν_4 that can be best explained by an effective D_2 crystal field for the ammonium ion (Table 1).

Rietveld refinement

Rietveld analyses were performed on two XRD spectra from selected samples of both the ammonioleucite and ND_4-ammonioleucite syntheses. In Fig. 5, the corresponding observed and calculated X-ray patterns are shown. The refined leucite yield was 74 wt.% in both runs (Table 3). Minor amounts of quartz, tobelite and buddingtonite were detected. The structures of ammonioleucite and ND_4-ammonioleucite were satisfactorily refined in space group $I4_1/a$. Statistical parameters for the refinements were within the range, which indicates a good fit (Table 3; cf., Harlov *et al.*, 2001*a,b*). Reflection positions and the relative intensities of the first 50 strongest peaks for synthetic ammonioleucite and ND_4-ammonioleucite are given in Table 4. No significant differences were observed compared to the reflection data from a natural (NH_4,K)-leucite refined by Hori *et al.* (1986).

Refined lattice constants for ammonioleucite and ND_4-ammonioleucite are listed in Table 5. In ammonioleucite (and ND_4-ammonioleucite), the NH_4^+ (ND_4^+) molecule replaces the K^+ cation in the leucite structure on the *W* site. The radius of NH_4^+ is 8% larger than K^+ ($r_{NH_4^+}$ = 1.43 Å, r_{K^+} = 1.33 Å for eightfold co-ordination). As a consequence, substitution of NH_4^+ for K^+ in the leucite structure results in an increase of the cell parameter *a* whereas the cell parameter *c* is slightly reduced. The mean <W–O> bond length of ammonioleucite is longer than in leucite from 3.00 Å (cf. Palmer *et al.*, 1997) to 3.12 Å, whereas the mean <*T*–O> bond length of 1.65 Å is unchanged.

The substitution of K^+ in leucite by the relatively larger Rb^+ and Cs^+ cations has been investigated by Palmer *et al.* (1997). A linear relationship between the cell parameters and the size of the *W* cation was observed. Figure 6 shows that the refined lattice constants and <*W*–O> distances of ammonioleucite are in good agreement with the observed trend for the K-Rb-Cs-leucite series as documented by Palmer *et al.* (1997). In general, the leucite structure consists of a framework of corner-sharing $(Al,Si)O_4$ tetrahedra which forms four-, six- and eight-member rings. Structural channels, parallel to the <111> direction, are formed by the arrangement of the six-member rings. These channels also represent the site on which the *W* cations are located. In K-bearing leucite, these six-member rings are normally distorted or crumpled. Substitution of Rb^+ or Cs^+ for K^+ on the *W* site in ammonioleucite results in less distortion of the channel structure (Palmer *et al.*, 1997). Here, the degree of crumpling in the six-member rings decreases as a function of the increasing size of the *W* cation as well as with increasing temperature. The Rietveld refinements reveal that the substitution of the NH_4^+ ion exhibits the same trend when hosting for K^+ on the *W* site in ammonioleucite.

This trend was also substantiated by the IR absorption spectroscopic measurements. At

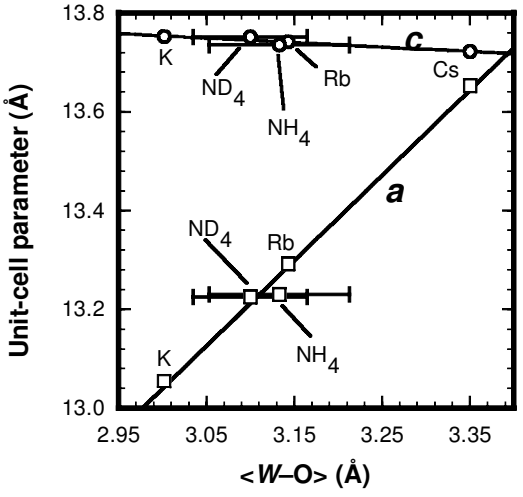

FIG. 6. Plot of variations in the lattice cell dimensions, *a* and *c*, for the mean <*W*–O> bond length for a series of substituted cations in leucite ($I4_1/a$). The K,Rb,Cs-leucite data are from Palmer *et al.* (1997). The ammonio- and ND_4-ammonioleucite data are from this study.

298 K, the *W* site, while comparably large, still represents a distorted crystal field, which causes some splitting of the vibrational bands of the ammonium ion. A decrease of the temperature to 77 K results in a smaller cavity and also in a more pronounced distortion of the channel structure. In turn, the crystal field surrounding the ammonium ion becomes stronger and more distorted. As a result, the T_d symmetry of the ammonium ion is lowered and the formerly triply degenerated vibrational bands split. At 77 K, the ν_4 band clearly appears to be splitting into three components, while the ν_3 band has evolved both a shoulder as well as substantial band broadening. Further possible features for ν_3 are hidden by combination bands. The ν_2 band remains IR inactive. These observations can best be explained by an effective crystalline field with a D_2 symmetry, i.e. a crystalline field with a higher symmetric than the respective site symmetry.

Acknowledgements

We thank Ursula Glenz and Helga Kemnitz for assistance with the SEM and Inka Bauer for help with sample preparation for both IR and XRD. M. Andrut gratefully acknowledges financial support through a research fellowship from the 'Fonds zur Förderung der wissenschaftlichen Forschung', Austria (project P13976-CHE). This project was supported by a German Science Foundation grant (He 2015-5) to Wilhelm Heinrich. We thank Mark Welch and an anonymous reviewer for their helpful and constructive comments which improved this manuscript.

References

Barrer, R.M., Baynham, J.W. and McCallum, N. (1953) Hydrothermal chemistry of silicates. Part V. Compounds structurally related to analcime. *Journal of the Chemical Society*, **1953**, 4035–4041.

Bastoul, A.M., Pironon, J., Mosbah, M., Dubois, M. and Cuney, M. (1993) In-situ analysis of nitrogen in minerals. *European Journal of Mineralogy*, **5**, 233–243.

Beran, A., Armstrong, J. and Rossman, G.R. (1992) Infrared and electron microprobe analysis of ammonium ions in halophane feldspar. *European Journal of Mineralogy*, **4**, 847–850.

Burgina, E.B., Yurchenko, E.N. and Paukshtis, E.A. (1986) Pecularities of the vibrational spectra of molecules adsorbed on the surface of heterogeneous catalysts: theoretical analysis. *Journal of Molecular Structure*, **147**, 193–201

Dollase, W.A. (1986) Correction of intensities for preferred orientations of the March model. *Journal of Applied Crystallography*, **19**, 267–272.

Griffiths, P.R. and de Haseth, J.A. (1986) Fourier Transform infrared spectroscopy. (*Chemical Analysis*, Vol. 83). Wiley, New York.

Harlov, D.E., Andrut, M. and Pöter, B. (2001*a*) Characterisation of buddingtonite $(NH_4)[AlSi_3O_8]$ and ND_4-buddingtonite $(ND_4)[AlSi_3O_8]$ using IR spectroscopy and Rietveld refinement of XRD spectra. *Physics and Chemistry of Minerals*, **28**, 188–198.

Harlov, D.E., Andrut, M. and Pöter, B. (2001*b*) Characterisation of tobelite $(NH_4)Al_2[AlSi_3O_{10}](OH)_2$ and ND_4-tobelite $(ND_4)Al_2[AlSi_3O_{10}](OD)_2$ using IR spectroscopy and Rietveld refinement of XRD spectra. *Physics and Chemistry of Minerals*, **28**, 268–276.

Herzberg, G. (1955) *Infra-Red and Raman Spectra of Polyatomic Molecules*. Van Nostrand, New York

Hori, H., Nagashima, K., Yamada, M., Miyawaki, R. and Marubishi, T. (1986) Ammonioleucite, a new mineral from Tatarazawa, Fujioka, Japan. *American Mineralogist*, **71**, 1022–1027.

Landolt-Börnstein, H. (1951) *Physikalisch-chemische Tabellen*, Vol. **2**. Edwards Brothers, Ann Arbor, Michigan, USA.

Larson, A.C. and von Dreele, R.B. (1987) *Generalized Structure Analysis System*. Los Alamos National

Laboratory Report No LA-UR-86-748, Los Alamos, New Mexico, USA.

Likhacheva, A.Yu., Paukshtis, E.A., Seryotkin, Yu.V. and Shulgenko, S.G. (2002) IR spectroscopic characterization of NH_4-analcime. *Physics and Chemistry of Minerals*, **29**, 617–623.

March, A. (1932) Mathematische Theorie der Regelung nach der Korngestalt. *Zeitschrift für Kristallografija*, **81**, 285–297.

Mertz, L. (1965) *Transformation in Optics*. Wiley, New York.

Nakamoto, K. (1986) *Infrared and Raman Spectra of Inorganic and Co-ordination Compounds*. Wiley, New York.

Nishida, N., Kimata, M., Kyono, A., Togawa, Y., Shimizu, M. and Hori, H. (1997) First finding of thallium-bearing ammonioleucite; a signal for the ultimate stage of the hydrothermal process and for a far-reaching effect from seawater alteration of MORB. *Annual Report of the Institute of Geoscience, University of Tsukuba*, **23**, 35–41.

Oxton, I.A., Knop, O. and Falk, M. (1975) Infrared spectra of the ammonium ion in crystals. I. Ammonium hexachloroplatinate (IV) and hexachlorotellurate (IV). *Canadian Journal of Chemistry*, **53**, 2675–2682.

Oxton, I.A., Knop, O. and Falk, M. (1976) Determination of the symmetry of ammonium ions in crystals from the infrared spectra of the isotopically dilute NH_3D+ species. *Journal of Physical Chemistry*, **80**, 1212–1217.

Palmer, D.C., Dove, M.T., Ibberson, R.M.and Powell, B.M. (1997) Structural behaviour, crystal chemistry, and phase transitions in substituted leucite: High-resolution neutron diffraction studies. *American Mineralogist*, **82**, 16–29.

Plumb, R.C. and Hornig, D.F. (1950) Infrared spectrum, X-ray diffraction pattern, and structure of ammonium fluoride. *Journal of Chemical Physics*, **23**, 947–953.

Wagner, E.L. and Hornig, D.F. (1950) The vibrational spectra of molecules and complex ions in crystals. III. Ammonium chloride and deutero-ammonium chloride. *Journal of Chemical Physics*, **18**, 296–304.

Yamada, M., Miyawaki, R., Nakai, I., Izumi, F. and Nagashima, K. (1998) A Rietveld analysis of the crystal structure of ammonioleucite. *Mineralogical Journal (Japan)*, **20**, 105–112.

[*Manuscript received 28 May 2003: revised 10 September 2003*]